DOI: 10.22226/2410-3535-2018-4-468-472 PACS: 81.05.Zx

Effect of the hatching strategies on mechanical properties and microstructure of SEBM manufactured Ti-6Al-4V specimens

V. V. Popov Jr.[1,†], A. Katz-Demyanetz[1], A. Kovalevsky[1], R. Biletskiy[1], E. Strokin[1], A. Garkun[1], M. Bamberger[2]

[†]vvp@technion.ac.il

[1] Israel Institute of Metals, Technion R&D Foundation, Technion City, Haifa 3200003, Israel
[2]Department of Materials Science and Engineering, Technion — Israel Institute of Technology, Technion City, Haifa 3200003, Israel

Powder Bed Additive Manufacturing is a relatively novel 3D-printing method of fabrication metallic components predominantly working with pre-alloyed powders. Laser or electron beam melt the powder in each layer according to the cross-section of the printed model. The combination of freedom of design and high mechanical properties of resulting material make PB-AM popular for different industrial applications including biomedical implants and aerospace part production. Titanium alloys and especially Ti-6Al-4V are among the most popular materials for additive manufacturing. It is mainly due to its high strength to weight ratio, biocompatibility, and high fatigue and corrosion resistance. Selective electron beam melting is already well-known effective additive manufacturing technology for wide range of applications. The high mechanical properties are provided due to vacuum environment of the process and specific temperature conditions. The final microstructure and required properties could be controlled by the adjustment of internal process parameters such as beam power (BP), beam scan rate (BR), hatching distance (HD) — distance between beam traces, and layer thickness (LT). In the current research the hatching strategy for SEBM manufacturing of Ti-6Al-4V was optimized and its influence on the mechanical properties and microstructure of the resulting components was analyzed. It was found that optimized HD with additional proper placement of components on the start platform can help to shorten the lead time without compromising the mechanical properties.

Keywords: additive manufacturing, hatching distance, selective electron beam melting, SEBM, Ti-6Al-4V.

1. Introduction

Selective Electron Beam Melting (SEBM) is a promising powder bed additive manufacturing (PB-AM) process for manufacturing near net-shape parts made of Titanium based alloys. Microstructure formation of molten metallic alloys, namely — nucleation and growth of various phases, depends among other factors on a thermal regime during and after the solidification [1]. Therefore, the adjustment of SEBM parameters is an effective instrument for microstructure handling, predicting mechanical properties of manufactured parts and regulating the component manufacturing time [2 – 3]. In SEBM process the high power electron beam, focused by electromagnetic lenses melts the powder layers according to the build file using chosen parameter settings including the scanning strategy related ones [2]. The main elements of beam scanning strategy in SEBM are contouring and hatching. In contouring the beam melts the outline of cross-section of each component and it defines the component surface properties. During hatching the beam melts the areas of solid metal "filling in" the contour [4]. SEBM process developed by ARCAM EBM [5] takes place at an elevated temperature. High temperature process conditions result in lower residual stress of the components manufactured by this technology. SEBM is carried out in vacuum environment as compared to the inert gas atmosphere with laser based additive manufacturing resulting in lower porosity level, increasing the density of SEBM-manufactured material up to 99.8% and better. The type of porosity of SEBM-parts also differs from that in laser manufactured ones, because the pores generated during the process are "vacuum-filled" rather than gas-filled ones in the case of laser-based PB-AM. Tammas-Williams et al. [4] reported that the melt strategies strongly affect the residual defects population in Ti-6Al-4V SEBM manufactured parts. The process parameters and optimized hatching and contouring strategies strongly affect the porosity level and distribution of defects, and can improve the fatigue resistance of the printed components.

Scharowsky et al. [6] reported and discussed the influence of hatching strategy on material consolidation during SEBM of Ti-6Al-V. The authors presented various process maps as combinations of beam power and scan speed parameters for a range of hatching distances between 20 and 200 μm. They also concluded that with the scan speeds smaller than a certain critical one result in significant heat diffusion into the part from the processed layer, whereas at higher scan speeds, heat of previous lines is still present at the interaction zone. Thus, for small scan speeds, high beam energies are necessary to achieve a good melting of the entire powder layer.

Murr [7] and Umaras et al. [8] mentioned a great importance of melting strategy in forming desired microstructure of the as-built metallic components.

Smith et al. analyzed and reported effect of dimensional inaccuracy of SEBM on defects in AM manufactured Ti-6Al-4V made parts [9]. The authors presented modified set of process parameters, including the decreased beam energy density, increased beam rate, and reduced contour energy that finally provided improved dimensional accuracy. On the other hand, reducing the energy density caused an increase in the number and size of the pores generated due to a lack of fusion in localized regions.

The work of Pushilina et al. is also devoted to the effect of SEBM process parameters on microstructure of Ti-6Al-4V components [10]. Additionally the authors investigated hydrogen sorption during the modified SEBM process. The process parameters chosen for investigation were beam current and beam scan rate.

Antonysamy et al. investigated the difference between the microstructure of contour and hatch areas in the titanium components manufactured using electron beam [11]. The authors describe the effect of beam hatching on propagation of coarse grain columnar β-fiber textured structure parallel to the build direction. However in the contour areas forming surfaces of bulk component more complex grain structure was observed.

Wang et al. considered the fusion conditions between the contour and hatchareas for optimization of the process parameters influencing surface roughness through AM of Ti-6Al-4V made components [12]. Different contouring strategies (including continuous beam contouring and so-called "multispot" ones, when beam is constantly jumping through the contour line allowing for better heat dissipation) were investigated. The main conclusion was that the "multispot" strategy results in better dimensional accuracy together with higher surface roughness. At the same time the continuous beam contouring has opposite effect decreasing dimension accuracy and lowering surface roughness.

Markl et al. developed a numerical method and have performed a simulation of SEBM process and compared the simulated results with experimental ones. The authors concluded that modified scan strategies are able to use the potential of future electron beam guns with higher powers to decrease the build time, reduce manufacturing costs and extend the variety of possible applications [13]. The authors also mentioned that improved process can be achieved using many other parameters like layer thickness, beam power, or size and distribution of powder particles.

Based on the recent works mentioned above, it must be concluded that optimization of the SEBM process parameter setting is a multidimensional task (multiple parameters influence the process, and some of them may be coupled together) strongly dependent on the optimization goal. In general, increase of the hatching distance reduces the manufacturing time, but may cause lack of fusion defects. However, significant decrease in HD can lead to local overheating causing stronger element evaporation, additional porosity and "swelling" on the surface layers. Thus, the engineering task is to find the optimal balance between relevant parameters reducing manufacturing still providing adequate mechanical properties of the components. The present paper reports practical results and then discusses the influence of HD, which is considered as a distance between two adjacent beam lines, on the obtained microstructure and mechanical properties of the SEBM Ti-6AL-4V parts aiming at finding better scanning strategies.

2. Experimental setup

The Ti-6Al-4V precursor powder with a particle size distribution of 45 – 120 μm, supplied by Arcam EBM© (Sweden), was used for the research. The restriction on the minimum particle size ensures safe handling of the powder. Usage of more dispersed powders (with smaller average diameter) can result in the process instability, and cause risks of explosion in handling. The coarser powders potentially can be used, but changes in the powder particle size distribution may need additional process parameter changes, and can cause undesired effect on the material microstructure. The fraction of finer particles and small satellites must be reduced, because they can cause considerable reduction of flowability, density and electric conductivity of the powder. The powder used for the printing was of the same quality (15 – 18 recycling), and no degradation of morphology and particle dispersion was observed as compared to the virgin powder.

Arcam A2X EBM© machine under vacuum below 1.5×10^{-4} mBar was used to carry out the electron beam melting process. Arcam A2X is an industrial machine designed for processing of titanium alloys, as well as materials that require high temperatures during melting. Overall build area envelope is $200 \times 200 \times 380$ mm.

Three sets of prismatic components with rectangular cross section were manufactured by SEBM to investigate the microstructural effect of HD change in three separate builds. In each build dimensions of the samples was the same: 10×10 mm in cross section and 100 mm in height. Each build contained six groups of 9 components, each group manufactured with different hatching distances of 100, 200, 300, 400, 500 and 600 μm (Fig. 1). Three builds differed from each other by the distances between the prisms in the groups: 10 mm between the samples in all groups in build 1, and 5 and 2 mm between the prisms — in builds 2 and 3. Such arrangement of samples on the start plate allows evaluating the influence of both HD and the gap between printed parts. In all cases beam current was kept the same 15 mA.

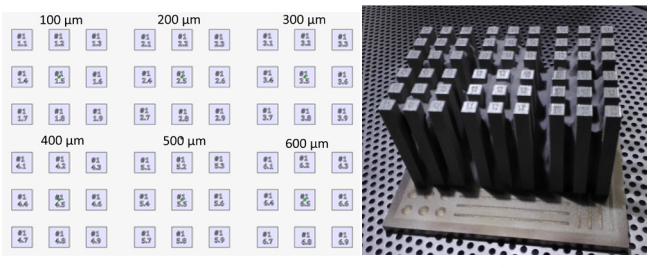

Fig. 1. Start plate 210×210 mm with 54 prismatic Ti-6Al-4V SEBM specimens arranged as 6 groups of 3×3: schematic view (a), image of the printed samples (b).

Microstructure and mechanical properties of all as-built samples were analyzed.

Additional experiments involved manufacturing the samples with strongly reduced HD of 80 and 50 μm, with spacing between parts 10 mm in the build #4.

Samples for electron microscopy investigation were cut from samples at mid-height to avoid the influence of differences in thermal regimes at the start and finish of the build.

3. Results and discussion

3.1. Microstructure examination

The microstructure of the as-built SEBM specimens is shown in Figs. 2 – 4 and S1 (supplementary material). It may be seen (see Fig. 2a – d), that increasing hatching distance leads to finer material microstructure due to smaller sample overheating. On the other hand, (see Fig. 2e – h), material porosity is increasing with increasing HD, mainly because of larger numbers of lack of fusion defects. The same trend with changing HD is observed for all distances between the samples (10 mm distances — Fig. 2, 5 mm distances — Fig. S1, 2 mm distances — Fig. 3). The same time microstructure of the samples manufactured with smaller spacing between them is coarser (Fig. 2a – d and Fig 3a – d).

Decreasing the HD from to 80 and then to 50 μm caused further coarsening of material microstructure (build #4, see Fig. 4), which might negatively affect mechanical properties of the as-printed product. But the same time amount of lack of fusion defects is significantly decreased, which is probably due to the consecutive remelting of adjacent traces and consecutive layers.

It must be noted that too small HD (less than ~100 μm), as well as too small gap (less than ~2 mm) result in the similar microstructure (see Figs. 3a, 4b, 4c) to the one obtained through hot isostatic pressing (HIP) of as manufactured Ti-6Al-4V parts, as reported in [14 – 15]. The HIPed-like microstructure results in similar material's mechanical properties.

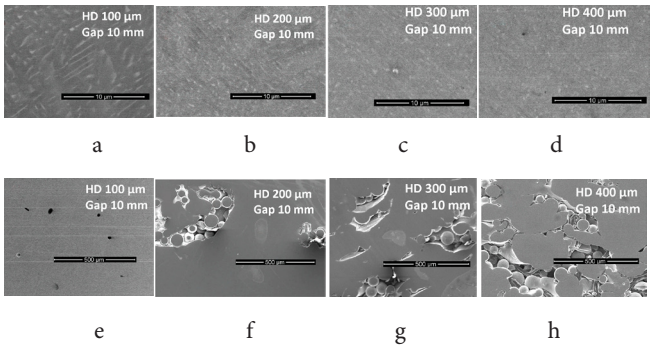

Fig. 2. Ti-6Al-4V SEBM manufactured samples from set #1 (10 mm distance between parts). Backscattered electron images of the microstructure with: HD = 100 μm (a); HD = 200 μm (b); HD = 300 μm (c); HD = 400 μm (d). SEM-images showing typical defects: HD = 100 μm (e); HD = 200 μm (f); HD = 300 μm (g); HD = 400 μm (h).

3.2. Mechanical properties evaluation

Mechanical properties of as-printed samples were examined using Instron 8802 mechanical testing machine by Illinois Tool Works Inc. (load cell SN 304606 with loading range up to 250 kN, extensometer for measuring from 0 to 12.5 mm). For mechanical properties samples with diameter of 6 mm were machined from as-manufactured by SEBM prisms according to ASTM E1012 Standard. Parallel length for measuring sample elongation was 40 mm; ramp rate used was 0.005 mm/min^{-1} until 2% deformation and 1.0 mm/min after 2% deformation.

It may be seen, that the samples printed with the lower (until 100 μm) HD (see Table S1, supplementary material) demonstrate the better mechanical properties (tensile strength, yield, cross-sectional reduction of area and elongation). Increasing the HD up to 400 μm caused, first of all, degradation in reduction of area and elongation, most possibly, due to the larger number of lack of fusion defects and poor material consolidation. Decreasing the distance

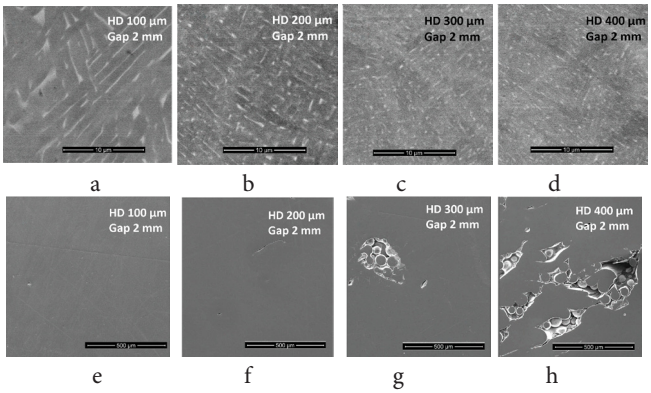

Fig. 3. Ti-6Al-4V SEBM manufactured samples from set #3 (2 mm distance between parts). Backscattered electron images of the microstructure with: HD = 100 μm (a); HD = 200 μm (b); HD = 300 μm (c); HD = 400 μm (d). SEM-images showing typical defects: HD = 100 μm (e); HD = 200 μm (f); HD = 300 μm (g); HD = 400 μm (h).

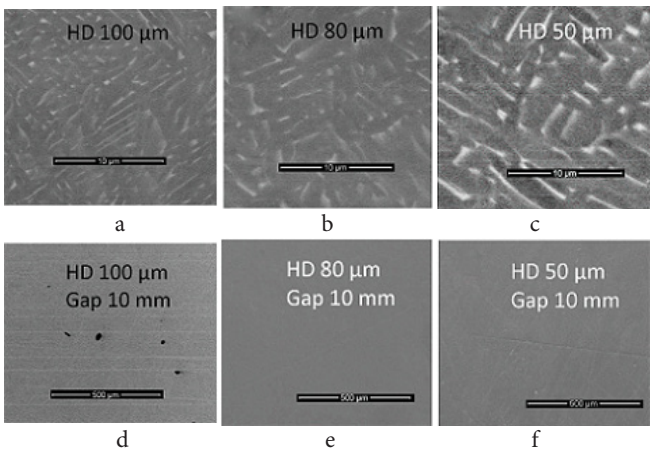

Fig. 4. Microstructure of Ti-6Al-4V SEBM manufactured samples from set #4. Backscattered electron images of the microstructure with: HD = 100 μm (a); HD = 80 μm (b); HD = 50 μm (c). SEM-images showing typical defects: HD = 100 μm (d); HD = 80 μm (e); HD = 50 μm (f).

between the as-printed parts results in improvement in tensile properties. It can be explained by their mutual heating that provides homogeneously consolidated microstructure.

On the other hand, decreasing the HD down to 50 μm caused degradation in mechanical properties (see Table S2), most probably, due to overheating of the material.

3.3. Microhardness

Microhardness measurements were carried out in 20 – 25 randomly selected points on each of polished surfaces at room temperature using Buehler Micromet 2004 (Switzerland) hardness tester. The hardness values for the different HD were found to be similar for all samples tested. The Vickers hardness HV ranged from 345 ± 18 HV for all samples.

3.4. Fractographic examination

Fracture surfaces of the broken tensile samples manufactured in different builds (different distances between prisms 10, 5 and 2 mm) and different HD (100, 200 and 300 μm) are shown in Figs. 5 and S2 – 9. The fracture surfaces investigation was carried out using Scanning Electron Microscope FEI Quanta 200 Inspect (SEM) by FEI Company, USA.

All figures labeled "a" present typical micrographs with low magnification (×100) demonstrating the overall structure of the fracture surfaces. All figures labeled "b" present typical structures of the fracture surfaces at high magnifications (×1000).

Comparing the brake surface structures from the samples manufactured with different hatching distances, namely the samples printed with HD 100 μm (Figs. S2a, S4a, S7a), HD 200 μm (Figs. 5a, S5a, S8a) and HD 300 μm (Figs. S3a, S6a, S9a), it is clear that the tendency to form lack of fusion defects increases with increasing HD. On the other hand, for the samples manufactured with the same HD but with different distance between the prisms, lack of fusion defect density decreases with decreasing distance between the samples indicating better material consolidation. In the extreme case of large hatching distances (300 μm) with large prism spacing (build #1, 10 mm) areas with virtually unchanged powder grains surrounded by solidified material are visible on the tensile sample brake surface (see Fig. S3a). And though samples manufactured with HD 300 μm and smaller prism spacing of 5 and 2 mm and are consecutively denser they still have large amount of lack of fusion defects resulting in poor material consolidation (Fig. S9a).

Large HD together with large spacing between the samples in the build most probably results in lower average temperatures of the upper layers of the parts and thus increased numbers of different lack of fusion defects causing the lack of material plasticity.

The images presenting a highly magnified fracture surfaces are also evidencing the effects mentioned above (see Figs. 5b, S3b, and S6b). Only the in the samples printed with low HD and small distance between the components in the build the typical plastic dimples are seen at their fracture surfaces (see Figs. S2b, S4b, S5b, S7b, S8b, S9b).

3.5. Sintered powder examination

The specific feature of SEBM process is that the powder surrounding the printed component is semi-sintered (see Fig. 6a – b). As the result of the sintering thin "bridges" between the powder grains are formed [16]. The coupling between the properly sintered powder grains is relatively easily broken during powder recycling. But in the case of powder overheating its recovery may become problematic, and significant change in the powder microstructure may cause changes in the properties of the material manufactured from such powder. Decreasing the distance between components together with the increased HD can result in smaller manufacturing times. However, additional powder heating between closely spaced solid components can cause its overheating with a potential of constraining recycling and further powder use.

SEM investigation of semi-sintered powder recovered from the gap between the components at the middle height showed that there is no significant effect on powder

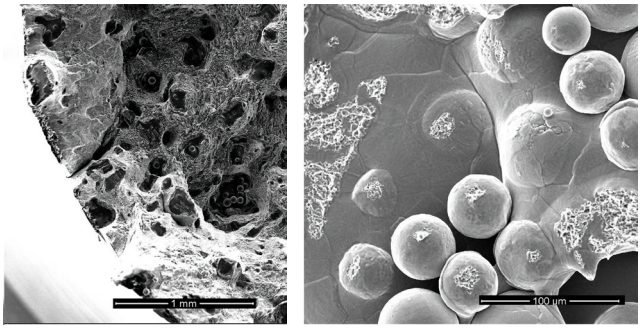

Fig. 5. SEM-images on the fractured surface: with low (×100, a); and high (×1500, b) magnification. Set #1: gap 10 mm between the prisms on the start plate, HD = 200 μm.

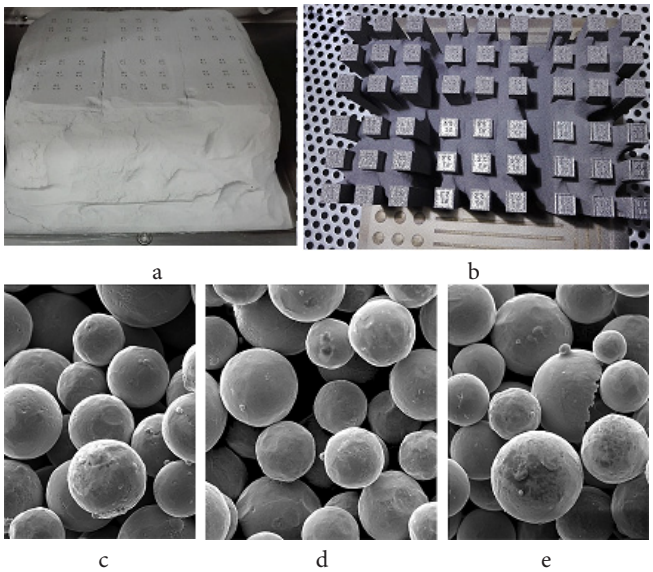

Fig. 6. Solid samples surrounded by the semi-sintered powder as coming from the build chamber (a) and after the powder is partially cleaned in the ARCAM Powder Recovery System (b); SEM images of the semi-sintered powder from the set #1 (10 mm gap between components) (c); set #2, gap — 5 mm (d); set #3, gap — 2 mm (e).

morphology caused by increased temperature (Fig. 6c – e). Nevertheless, deeper analysis (see Fig. 7) showed that specific bridges form between particles in the overheating conditions. Bonded powder particles may still pass the sieve and some of them may still remain after powder recovery process. Such particles bonding may decrease the flow ability of the reused powder, and cause the increased porosity in the components manufactured by SEBM [17].

4. Conclusion

Hatching distance strategy strongly affects microstructure and mechanical properties of as-printed SEBM manufactured components due to variations in the applied heating regimes. Decrease of the hatching distance causes the better component heating, better material consolidation and lower level of porosity. On the other hand, microstructure of the material can become coarser due to higher acting temperatures caused by smaller hatching distances and close spacing of adjacent components in the build. In case of serious overheating it may cause significant undesired impact upon the mechanical properties of resulting material.

Distance between the parts through printing may also affect the heating regime. And though by decreasing the spacing between adjacent components in the build it is possible to work with larger hatching distances and reduce the overall build time, undesirable microstructure coarsening due overheating may occur leading to worthier mechanical properties of the resulting material.

Based on the mentioned above, it may be concluded that HD strategy should be optimized and adjusted taking into account thermal properties of the used material and geometry of the printed parts.

Future research should be focused on application of the HD printing strategy established in the present paper to manufacturing certain critical aerospace parts made of Ti-6Al-4V alloy.

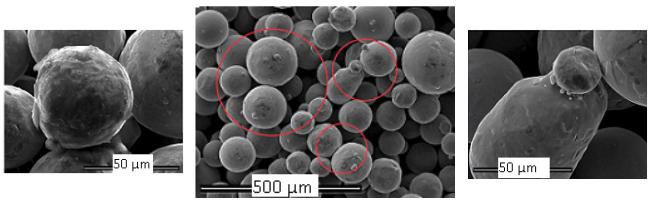

Fig. 7. SEM-image of semi-sintered powder from the gap between the parts (set #3 with 2 mm gap).

Acknowledgements. The present research was performed as a part of AATID Consortium program. The authors want to thank for support and advice Dr. Lucy Edery-Azulay, Lior Zilberman and Haim Rosenson. For access to original data and additional information, please contact the corresponding author.

Supplementary Material. *The on-line version of this paper contains supplementary material available free of charge at the journal's Web site (www.lettersonmaterials.com).*

References

1. V. Popov, A. Katz-Demyanetz, M. Bamberger. Defect Diffus. Forum. 383, 190 (2018). DOI: 10.4028/www.scientific.net/DDF.383.190
2. T. DebRoy, H.L. Wei, J.S. Zuback, T. Mukherjee, J.W. Elmerb, J.O. Milewski, A.M. Beese, A. Wilson-Heid, A. De, W. Zhang. Progress in Materials Science. 92, 112 (2018). DOI: 10.1016/j.pmatsci.2017.10.001
3. L.-E. Rännar, A. Koptyug, J. Olsén, K. Saeidi, Z. Shen. Additive Manufacturing. 17, 106 (2017). DOI: org/10.1016/j.addma.2017.07.003.
4. S. Tammas-Williams, H. Zhao, F. Léonard, F. Derguti, I. Todd, P.B. Prangnell. Mater. Charact. 102, 47 (2015). DOI: 10.1016/j.matchar.2015.02.008
5. Arcam EBM® AB, machines manufacturer, official web-site: http://www.arcam.com
6. T. Scharowsky, A. Bauereiß, C. Körner. Int.J. Adv. Manuf. Technol. 92, 2809 (2017). DOI: 10.1007/s00170-017-0375-1
7. L.E. Murr. Additive Manufacturing. 5, 40 (2015). DOI: 10.1016/j.addma.2014.12.002
8. E. Umaras, Marcos S.G. Tsuzuki. IFAC PapersOnLine. 50 – 1, 14940 (2017).
9. C.J. Smith, F. Derguti, E. Hernandez Nava, M. Thomas, S. Tammas-Williams, S. Gulizia, D. Fraser, I. Todd. J. Mater. Process. Technol. 229, 128 (2017).
10. N. Pushilina, M. Syrtanov, E. Kashkarov, T. Murashkina, V. Kudiiarov, R. Laptev, A. Lider, A. Koptyug. Materials. 11, 763 (2018).
11. A. Antonysamy, J. Meyer, P.B. Prangnell. Mater. Charact. 84, 153 (2013).
12. P. Wang, W.J. Sin, M.L. S. Nai, J. Wei. Materials. 10, 1121 (2017). DOI: 10.3390/ma10101121
13. M. Markl, R. Ammer, U. Rude, C. Körner. Int.J. Adv. Manuf. Technol. 78, 239 (2015). DOI: 10.1007/s00170-014-6594-9
14. K. Frisk, N. Petterson, D. Persson, L.-E. Rännar, A. Koptyug, A. Leicht, M.V. Sundaram, E. Hryha, L. Nyborg, M. Ahlfors. World PM 2016 Congress and Exhibition. (2016).
15. V. Popov, A. Katz-Demyanetz, A. Garkun, G. Muller, E. Strokin, H. Rosenson. Procedia Manufacturing. 21, 125 (2018). DOI: 10.1016/j.promfg.2018.02.102
16. A. Koptyug, L.-E. Rännar, M. Bäckström, R. Surmenev. Journal Nanotechnology: development and applications — XXI Century. 4, 12 (2016). DOI: http://www.radiotec.ru/article/18802
17. V.V. Popov Jr., A. Katz-Demyanetz, A. Garkun, M. Bamberger. Additive Manufacturing. 22, 834 (2018). DOI: 10.1016/j.addma.2018.06.003